Ann. Geophysicae 14, 865–878 (1996)

Annales Geophysicae

On the longitudinal extent of magnetopause reconnection pulses

M. Lockwood, C. J. Davis

Rutherford Appleton Laboratory, Chilton, Oxfordshire, UK

Received: 17 November 1995/Revised: 22 April 1996/Accepted: 25 April 1996

Abstract. The open magnetosphere model of cusp ion injection, acceleration and precipitation is used to predict the dispersion characteristics for fully pulsed magnetic reconnection at a low-latitude magnetopause X-line. The resulting steps, as would be seen by a satellite moving meridionally and normal to the ionospheric projection of the X-line, are compared with those seen by satellites moving longitudinally, along the open/closed boundary. It is shown that two observed cases can be explained by similar magnetosheath and reconnection characteristics, and that the major differences between them are well explained by the different satellite paths through the events. Both cases were observed in association with poleward-moving transient events seen by ground-based radar, as also predicted by the theory. The results show that the reconnection is pulsed but strongly imply it cannot also be spatially patchy, in the sense of isolated X-lines which independently are intermittently active. Furthermore they show that the reconnection pulses responsible for the poleward-moving events and the cusp ion steps, must cover at least 3 h of magnetic local time, although propagation of the active reconnection region may mean that it does not extend this far at any one instant of time.

1 Introduction

Three types of signature have now been identified which are strong candidates for signatures of pulsed magnetic reconnection at the Earth's magnetopause: (1) characteristic electric and magnetic field and particle signatures at the magnetopause called flux transfer events (FTEs); (2) poleward-moving auroral (630 nm dominant) transients (largely caused by enhancements in ionospheric electron temperature produced by magnetosheath-like electron precipitation) and, when the B_y component of the interplanetary magnetic field (IMF) is large, associated with strong transient east/west flow channels; (3) steps in cusp ion dispersion characteristics. In all three cases, debate has arisen about the spatial structure of the reconnection and the extent to which it is "patchy" as well as "sporadic".

1.1 Flux transfer events

The association of spatial and temporal variability in the magnetopause reconnection rate (i.e. patchy with sporadic reconnection) originates with the discovery of flux transfer event signatures (see Russell and Elphic, 1978). For many years, these signatures were interpreted in terms of a passage of a small circular flux tube over (or nearby to) the satellite, such a tube being produced by a burst of reconnection along a short X-line. In this context, short means of order 1 Earth radius (1 R_E) which, for a magnetopause at 12 R_E from the Earth, covers a range in magnetic local time (MLT) of order 0.25 h. However, in recent years there has been increased awareness that the FTE signature is dragged over the satellite, so no information on the dimension of the event normal to the direction of motion is obtained. Following suggestions by Saunders (1983), Biernat *et al.* (1987) and Southwood *et al.* (1988), FTE signatures have been reproduced both by numerical simulations (Scholer, 1988) and analytic theory (Semenov *et al.*, 1992) which are two-dimensional in nature and which do not specify what happens in the third dimension. As a result, magnetopause FTE signatures are now usually interpreted as revealing temporal variations in reconnection rate at one point on the reconnection X-line (Hapgood and Lockwood, 1995), but the spatial extent of the pulse of enhanced reconnection is not known. This is because any field lines opened at other points on the same X-line do not evolve over the satellite (Lockwood *et al.*, 1995). Similarly there is no knowledge about the existence or behaviour of other X-lines. However, patchiness of the reconnection is still frequently associated with its pulsed nature in time (e.g. Newell and Meng, 1991; Pinnock *et al.*,

Correspondence to: M. Lockwood

1995). Indeed Newell and Sibeck (1993) argued that there are theoretical limits on both the individual event size and their contribution to the transpolar voltage. These limits have been challenged by Lockwood *et al.* (1995a).

1.2 Poleward-moving transients

In recent years, this debate has been given impetus by ground-based optical observations of poleward-moving transients in the cusp/cleft region, with dominant 630 nm luminosity. Such emissions are predominantly generated by enhanced ionospheric electron temperatures produced by the precipitation of magnetosheath-like electrons (see discussion by Lockwood *et al.*, 1993b). These are thought to be another signature of pulsed magnetopause reconnection (see review by Sandholt *et al.*, 1992). The observations are made from either one or several observing stations and often indicate events which have large spatial dimensions. The term large in this context is applied to events above about 1000 km in longitudinal extent which corresponds to the order of 3 h in MLT. However, interpretation of the images is not unambiguous. One problem is that the images are line-of-sight luminosity integrations and the altitude profile of the 630 nm volume emission rate of the atomic oxygen is not known in detail. Other problems are caused by the smearing effect of thermospheric winds which move the excited atomic oxygen during the relatively long (and variable) radiative lifetimes between excitation and decay. The effects on the inferred event sizes were discussed by Lockwood *et al.* (1993b). They concluded that the events were longitudinally extensive by comparisons with simultaneous measurements of the latitudinal width by the EISCAT radar which were not subject to these uncertainties. This reasoning was not accepted by Newell and Sibeck (1993), who argued both longitudinal and latitudinal dimensions were smaller by a factor of about 6, for which the voltage contribution of each event is smaller by a factor of 36.

Lockwood *et al.* (1989) reported that these transient red-line auroral events in the Northern Hemisphere were coincident with transient westward flow bursts when the IMF has a strong positive B_y component. The flow velocity within the event was found to be roughly the same as the phase motion of the red-line event, a key signature of the ionospheric signature of a flux transfer event (Southwood, 1987). Later observations showed that negative B_y gave eastward flow bursts and event motion (Sandholt *et al.*, 1992; Lockwood *et al.*, 1993b; 1995b). This B_y-dependent motion is another key prediction for FTE signatures, as is the fact that the east/west motion evolves into poleward motion as the curvature ("tension") force on the newly opened field lines decays. On just one occasion joint observations have allowed an association to be made with magnetopause FTE signatures (Elphic *et al.*, 1990; Sandholt *et al.*, 1992). A further indication that there is a relationship between the two phenomena is the similarity of the distributions of the repeat periods (Lockwood and Wild, 1993; Fasel, 1995). Lockwood *et al.* (1990a) calculated that the events reported by Lockwood *et al.* (1989) must be longitudinally extensive (over 1000 km) from their lifetime at the observed meridian and from the observed westward flow speeds. They also deduced this large east-west extent from the lack of strong return flows outside the event. Direct observations that these flow bursts were indeed elongated flow channels was provided by Pinnock *et al.* (1993) who detected such an event which was at least 900 km long in the extended field of view of the Halley Bay HF radar. The Pinnock *et al.* (1993) results also provided a firm link between the flow transients and the cusp precipitation, as had been inferred by Lockwood and Smith (1989), as part of the pulsating cusp model. Other discussions about the size, voltage and significance of the poleward-moving auroral forms and associated flow channels on the dayside are given in Denig *et al.* (1993); Lockwood and Cowley (1994) and Moen *et al.* (1995; 1996).

1.3 Cusp ion steps

Discontinuities ("steps") in the dispersion of precipitating cusp ions were predicted theoretically by Cowley *et al.* (1991) and Smith *et al.* (1992), based on the model by Cowley and Lockwood (1992) of how ionospheric convection is excited. The cusp precipitation between the steps results from pulses of enhanced magnetopause reconnection, as suggested by Lockwood and Smith (1989). Independent of these theoretical considerations, Newell and Meng (1991) presented some examples of steps which were interpreted by Lockwood and Smith (1992) in terms of the pulsating cusp model. Other examples were presented and explained in terms of the pulsating cusp model by Escoubet *et al.* (1992) and Lockwood *et al.* (1993a).

Lockwood and Smith (1994) predicted that the form of the steps in field-aligned ions (on an energy-time spectrogram) will depend on the ratio of the components of the convection and satellite velocities which are normal to the open/closed separatrix (respectively V_c and V_s, both defined as positive poleward). In particular, for satellites moving meridionally poleward/equatorward at low altitudes (for which $V_s/V_c \gg 1$ and $\ll -1$, respectively), pulsed reconnection will produce up/down ramps in the cusp ion spectrogram, separated by up/down steps. Examples of these two cases have been reported by Lockwood and Smith (1989) and Lockwood *et al.* (1993a). For satellites moving longitudinally along the open/closed separatrix ($|V_s/V_c| < 1$), Lockwood and Smith (1994) predicted that the cusp ions will show downward ramps, separated by upward steps. This has recently been verified Pinnock *et al.* (1995). The condition $|V_s/V_c| < 1$ will often also apply for mid-altitude satellites and Lockwood and Smith (1994) argue that at least some of the overlapping injection signatures seen by the Viking satellite (Woch and Lundin, 1991; 1992) are in fact examples of such upward steps in field-parallel ions with gyroradius effects for the larger pitch angle ions.

Some observations of cusp ion steps have been interpreted as quasi-steady reconnection with spatial structure (Onsager *et al.*, 1995; Weiss *et al.*, 1995). However, it is clear that not all events can be explained this way. The theory of how time-varying reconnection produces cusp

ion steps also predicts that they will sit on the boundary between the poleward-moving events (see following section). Thus, the observations of cusp ion steps at the boundaries between poleward-moving events by Lockwood *et al.* (1993a) and Pinnock *et al.* (1995) are important confirmation of this theory. However, debate has arisen about the spatial extent of the events and the degree to which reconnection which is sporadic in time is also patchy in space. Indeed Pinnock *et al.* (1995) argue against two longitudinally separated features at low altitudes being the same event, specifically on the grounds that it would require the reconnection burst to cover a correspondingly large range of longitudes at the magnetopause. They interpret an isolated patch of magnetosheath-like precipitation, seen by the satellite as it moves longitudinally, as showing that the reconnection is spatially patchy as well as bursty in time.

In this study, we present illustrative model predictions of the ion spectrograms for cusp passes during which the reconnection takes place at the subsolar magnetopause, but only in a series of short pulses. Section 2 reviews the expected effects of such pulsed reconnection on the dayside magnetosphere-ionosphere system and Sect. 3 compares spatial and temporal origins of cusp ion steps. In Sect. 4, we describe how we make predictions of the observed cusp ions for satellites moving meridionally, normal to the open-closed boundary, and for satellites moving longitudinally along that boundary. The results are compared with the observations of cusp ion steps presented by Lockwood *et al.* (1993a) and Pinnock *et al.* (1995) in Sect. 5. It is shown that the major features of these two cases can be reproduced by the same simple model, their different character arising largely from the direction of the satellite motion. The model assumes that the events are longitudinally extensive and cover at least the MLT range of the satellite intersection with the cusp. In Sect. 6, we discuss how all the features seen by Pinnock *et al.* (1995), including the isolated patch of precipitation, can arise from temporal variations in the reconnection rate, with no need to invoke spatial structure.

2 The effects of pulsed reconnection

For completeness, this section presents a review of the basic concepts of the effects of pulsed magnetopause reconnection which has emerged in recent years and which is used in subsequent sections of this work. By definition, a pulse of reconnection during southward IMF conditions will produce a patch of newly opened flux in the ionosphere and a patch of rotational discontinuity on the magnetopause. Both these are threaded by the newly opened field lines and recent observations and theory give us an understanding of how both will evolve. This understanding leads to the prediction of FTE signatures, poleward moving events and cusp ion steps, as is explained in this section.

A model of how ionospheric convection is excited on short time scales by reconnection has been developed by Cowley and Lockwood (1992) from EISCAT-AMPTE observations of the response of dayside flows to changes in the magnetic shear across the dayside magnetopause (Todd *et al.*, 1998; Etemadi *et al.*, 1988; Lockwood *et al.*, 1990b). This model incorporates the theoretical concept of adiaroic polar cap boundaries introduced by Siscoe and Huang (1985) and the effects of their motions as employed by Freeman and Southwood (1988) to explain joint satellite and radar observations of the ionospheric signatures of magnetopause erosion.

On time scales short compared with several substorms cycles, the magnetospheric magnetic field cannot be considered constant. This means that induction effects are important and the electric field at the magnetopause does not simply map down field lines into the ionosphere, as it does in the steady-state limit (see discussion by Lockwood and Cowley, 1992). Note that this in no way implies the existence of electrostatic field-parallel electric fields. This concept has recently been discussed in various ways by several authors: a Faraday loop approach was adopted by Lockwood *et al.* (1990b) and Lockwood and Cowley (1992); however, similar conclusions emerge from the inductive electrical circuit analogy of Sanchez *et al.* (1991), based on the work of Holzer and Reid (1975); the line-tying concepts of Coroniti and Kennel (1973) and the separation of non-steady reconnection rate into potential and vortex components by Pudovkin *et al.* (1992). An important feature of inductive smoothing is that a short-lived pulse of magnetopause reconnection generates only a gradual rise and decay of flow in the ionosphere.

The reasons for this are demonstrated by Fig. 1 (after Lockwood, 1994). Each part of this figure presents a view of the magnetosphere from mid-latitudes and the mid-afternoon sector. AB is a magnetopause X-line, dy' long, which maps along magnetic field lines to an ionospheric merging gap ab (length dy). If we apply Faraday's law to the fixed loop ABba in the Earth's frame, with the assumption that field-parallel electrostatic fields can be neglected:

$$\oint_{\mathrm{ABba}} E \cdot dl = E_t\, dy' - E_i\, dy = d/dt\left(\int_{\mathrm{ABba}} B \cdot da\right) = dF/dt, \tag{1}$$

where E_t is the electric field along AB (here taken to be constant over the length dy') and E_i is the electric field along the merging gap ab (here assumed to be constant along the length dy for simplicity), both being measured in the Earth's frame of reference. F is the magnetic flux threading the Faraday loop ABba.

In Fig. 1a, the magnetosphere-ionosphere system is in steady-state, i.e. the X-line AB and the merging gap ab are both static in the Earth's frame and F is constant. In this case, the reconnection rate (i.e. the electric field ε along AB in its own rest frame) is equal to E_t and, from equation (1), $E_t\, dy'$ is equal to $E_i\, dy$. The electric field E_i drives flux poleward in the ionosphere and the shaded regions show where the newly opened flux produced by the reconnection thread the magnetopause and the ionosphere. In this case, the applied voltage $\varepsilon\, dy'$ all appears across the merging gap ab in the ionosphere. Figure 1b, however, shows the results if the reconnection is unable to move the ionospheric plasma (on short time scales this applies because of the drag produced by collisions of ions with the

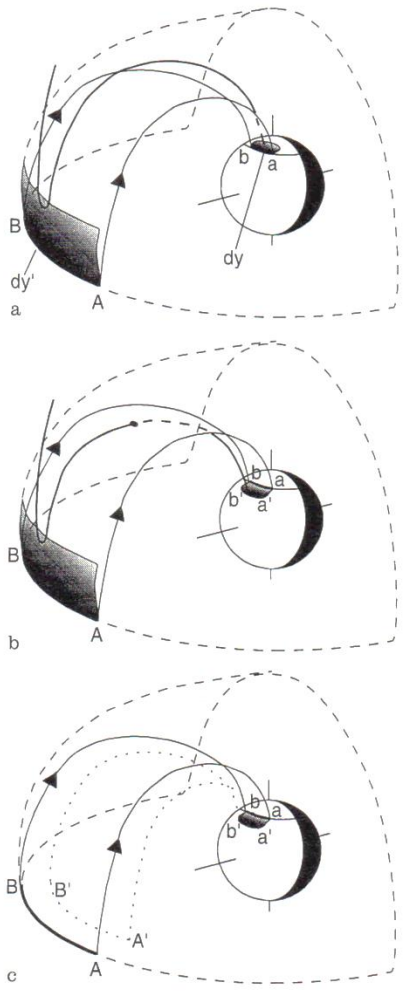

Fig. 1a–c. The possible effects of a reconnection pulse at a magnetopause X-line AB, which maps to an ionospheric merging gap ab. **a** is the steady-state case where ab and AB are static in the Earth's frame and there is no change in the magnetic field in the dayside magnetosphere. In this case, the newly opened field lines (like the one shown which thread the magnetopause and the ionosphere in the shaded regions) do not thread the Faraday loop $ABba$ and poleward flow is excited in the ionosphere in the Earth's frame by the reconnection rate. In **b** AB is static but ab migrates equatorward to $a'b'$ such that the newly opened field lines thread the Faraday loop $ABba$ to the extent that no flow is excited in the ionosphere in the Earth's frame. In **c** the X-line AB erodes Earthward to $A'B'$ and ab moves equatorward to $a'b'$, again exciting no ionospheric flow in the Earth's frame

much more numerous neutral particles). In this case, AB is again static in the Earth's frame so E_t is again equal to ε but ab now migrates equatorward to $a'b'$ such that all the newly opened flux threads the Faraday loop ABba. In this case dF/dt is equal to the applied voltage $\varepsilon\, dy'$, such that E_i is zero. In part (c) the magnetopause erodes Earthward such that the X-line migrates from AB to A'B'. This can occur at a speed such that the electric field in the Earth's frame E_t falls to zero, even though there is an applied electric field ε in the rest frame of the magnetopause: in this case both E_i and dF/dt are zero and the merging gap ab erodes equatorward as new open flux is generated.

In general, a mixture of all three processes can take place. Both the erosion (Fig. 1c) and induction (Fig. 1b) effects cause the voltage appearing in the Earth's frame of reference across the ionospheric merging gap to be less than that across the X-line in its rest frame (as it would be in the steady-state limit, Fig. 1a). However, in both cases, the open/closed boundary migrates equatorward in the Earth's frame, such that the flux transfer rate across the merging gap (i.e. the voltage in its rest frame) is equal to that across the X-line (in its rest frame).

The ionosphere is almost incompressible, in the sense that the magnetic field there, B_i, is approximately constant. Thus the reconnection rate (i.e. a tangential magnetopause electric field, ε) causes the growth in the area of newly opened flux in the ionosphere. From this the flow of frozen-in ionospheric plasma across the ionospheric merging gap, in its own rest frame, V', is given by (Lockwood and Smith, 1992):

$$V' = (\varepsilon/B_i)\cdot(dy'/dy). \tag{2}$$

The (poleward) boundary-normal plasma flow velocity across the merging gap, in its own rest frame, is V' but that in the Earth's frame is V_c: thus the boundary velocity (defined here as positive poleward) is (Lockwood *et al.*, 1993c):

$$V_b = (V_c - V'). \tag{3}$$

Consider two limits of the general behaviour: were it possible for the merging gap location to remain fixed in the Earth's frame ($V_b = 0$), then $V_c = V'$ – i.e. poleward plasma flow is seen in the Earth's frame (the situation in Fig. 1a). In the other limit, no flow is driven in the Earth's frame, but the boundary migrates equatorward, i.e. $V_c = 0$ and $V_b = -V'$ (the situation in Fig. 1b, c). Which of these two limits most closely resembles the actual behaviour is a matter of the time scale of the reconnection pulses. The time constant for exciting the full ionospheric flow depends on how quickly the ionosphere can be set into motion and, thus, on the frictional drag caused by the neutral thermosphere. This time constant has been estimated to be of the order of 15–20 min in a number of studies: it emerges from the inductive circuit analogies (Holzer and Reid, 1975; Sanchez *et al.*, 1991), from line-tying arguments (Coroniti and Kennel, 1973), from high-time resolution studies of the response of ionospheric flow to IMF B_z changes (Todd *et al.*, 1988; Etemadi *et al.*, 1988); and from the Cowley and Lockwood (1992) flow excitation model. The models and observations thus predict that ionospheric flow will commence following the onset of reconnection but only after the Alfvén wave arrives in the ionosphere (after an Alfvén transit time which is here taken to be 1 min); however, if the reconnection persists, this flow will subsequently increase over a period of 10–15 min. If the reconnection ceases soon after it commences, the short pulse in ε will be inductively smoothed to give a more gradual rise and then fall of ionospheric flow in the Earth's frame. Note that the

precise value of the smoothing time constant is not important here, other than it is larger than the reconnection pulse duration. In this study, we are concerned with reconnection pulses which are 1 min in duration. Hence during such pulses, the rise in ionospheric flow will be very small, i.e. $V_c \approx 0$ and $V_b \approx -V'$. Such equatorward motion of the ionospheric open/closed boundary in response to magnetopause reconnection is well known, even on longer time scales, and has been observed in cusp particle precipitation (Burch, 1973), the 630 nm emissions caused by that precipitation (Horwitz and Akasofu, 1977; Sandholt *et al.*, 1992) and radar studies of the cusp/cleft region (Foster *et al.*, 1980).

If, after such a pulse, there is a complete cessation of reconnection, then no flux will cross the open/closed boundary: to use the terminology introduced by Siscoe and Huang (1985), it becomes adiaroic (meaning not flowing across, $V' = 0$ and hence $V_c = V_b$). As we will discuss later, the boundary will, in fact, tend to return poleward ($V_b > 0$) and hence this generates poleward ionospheric flow ($V_c > 0$).

The model of Cowley and Lockwood (1992) gives a framework in which the evolution of the ionospheric flow can be understood. Following the work of Southwood (1987) and Freeman and Southwood (1988), these authors introduced the concept of zero-flow equilibria of the magnetosphere-ionosphere system for a given amount of open flux. This is an idealised concept because, in practice, some other source of flow is always likely to be present (viscous interaction, and/or lobe or tail reconnection); however, recent observations show that this concept is not merely an obscure abstraction. Knipp *et al.* (1993) have presented flow snapshots, derived by the AMIE technique, for both hemispheres during a period of prolonged northward IMF (similar results were derived for the same period by Freeman *et al.* (1993) using just the satellite plasma flow data). In the summer hemisphere, strong reverse convection was seen, revealing lobe reconnection and the presence of open flux. The winter hemisphere remained almost completely stagnant, despite the fact that it must contain as much open flux as the summer hemisphere. This hemisphere was shielded from lobe reconnection by the overdraped lobe (Crooker, 1992) and neither hemisphere shows any evidence of significant tail reconnection. In the absence of any reconnection perturbing the winter polar cap, it achieved a zero-flow equilibrium. This was despite the presence of open flux tubes which, outside the magnetosphere, experience the motional electric field of the magnetosheath flow, that electric field did not map to the ionosphere because of induction effects of the type discussed earlier.

The power of the zero-flow equilibrium concept is that it allows us to predict the evolution of the pattern of flow generated following a pulse of reconnection as the magnetosphere-ionosphere system tends towards a new equilibrium with the new amount of open flux. Hence we can qualitatively predict the flow that will be excited by a pulse, or a string of pulses, of magnetopause reconnection. This was done by Cowley *et al.* (1991) who investigated the ionospheric signatures of reconnection bursts, using the zero-flow equilibrium concept for both small or large IMF $|B_y|$.

Figure 2 illustrates the predictions of Cowley *et al.* (1991) for fully pulsed reconnection at the subsolar magnetopause, when the B_y component of the IMF is small (as presented by Lockwood, 1994). The figure comprises three columns of diagrams.

a. The left hand diagrams show noon-midnight sections of the dayside magnetopause. Only illustrative newly opened field lines are shown and the solid and dashed segments of the magnetopause are tangential (TD) and rotational (RD) field discontinuities, respectively. The dot denotes an active X-line at noon.

b. The diagrams in the middle column view the dayside magnetosphere from mid-latitudes in the mid-afternoon sector: here the dashed regions show the edges of patches of magnetopause RD produced by bursts of reconnection, where the newly opened field lines thread the magnetopause. (The dots mark the points at which the illustrative newly opened field lines thread the boundary). The segments of the equatorial magnetopause shown by thicker lines are active X-line segments where reconnection is taking place at that time.

c. The diagrams to the right of the figure are views looking down on the northern hemisphere ionospheric polar cap. Noon is to the top and dawn to the right. The solid lines with arrows are plasma flow streamlines, the solid but thin lines are adiaroic segments of the open-closed field line boundary and the thicker solid lines are active merging gap segments (which map to the active X-line segments shown in the middle panels). The dashed lines delineate regions of newly opened flux produced by discrete pulses of reconnection.

Consider reconnection which is entirely pulsed: the reconnection at any one MLT all occurs in pulses, here taken to be $dt = 1$ min in duration and repeating with a period of $T = 4$ min. The successive rows in Fig. 2 are for times which are 1 min apart. If we define the first reconnection pulse as beginning at time $t = 0$, row N of Fig. 2 shows the situation at time $t = N$ min.

The reconnection is envisaged as commencing at noon, and subsequently spreading tailward. From observations, the speed of this expansion in the ionosphere is initially about 10 km s^{-1}, but falls to about 1 km s^{-1} near dawn and dusk (Lockwood *et al.*, 1986, Todd *et al.*, 1988; Etemadi *et al.*, 1988; Saunders *et al.*, 1992; Lockwood *et al.*, 1993c).

In part 1a and 1b of Fig. 2 (hereafter referred to as Figs. 2(1a) and 2(1b), respectively), a region of rotational discontinuity, produced by the reconnection pulse, is seen emerging from the (still active) X-line at time $t = 1$ min. For a typical field line speed over the magnetopause (de Hoffman-Teller velocity) of 320 km s^{-1}, these newly opened field lines migrate tailwards at 3 R_E per minute. In Fig. 2(1c), this newly opened flux forms an extrusion of the polar cap boundary. The main effect of the reconnection is to move the open-closed boundary equatorward ($V_b < 0$) but some weak poleward flow ($V_c > 0$) is just commencing, as the Alfvén wave arrives in the ionosphere.

At this time $t = 1$ min, the reconnection at noon switches off and this switch-off will expand tailward in the

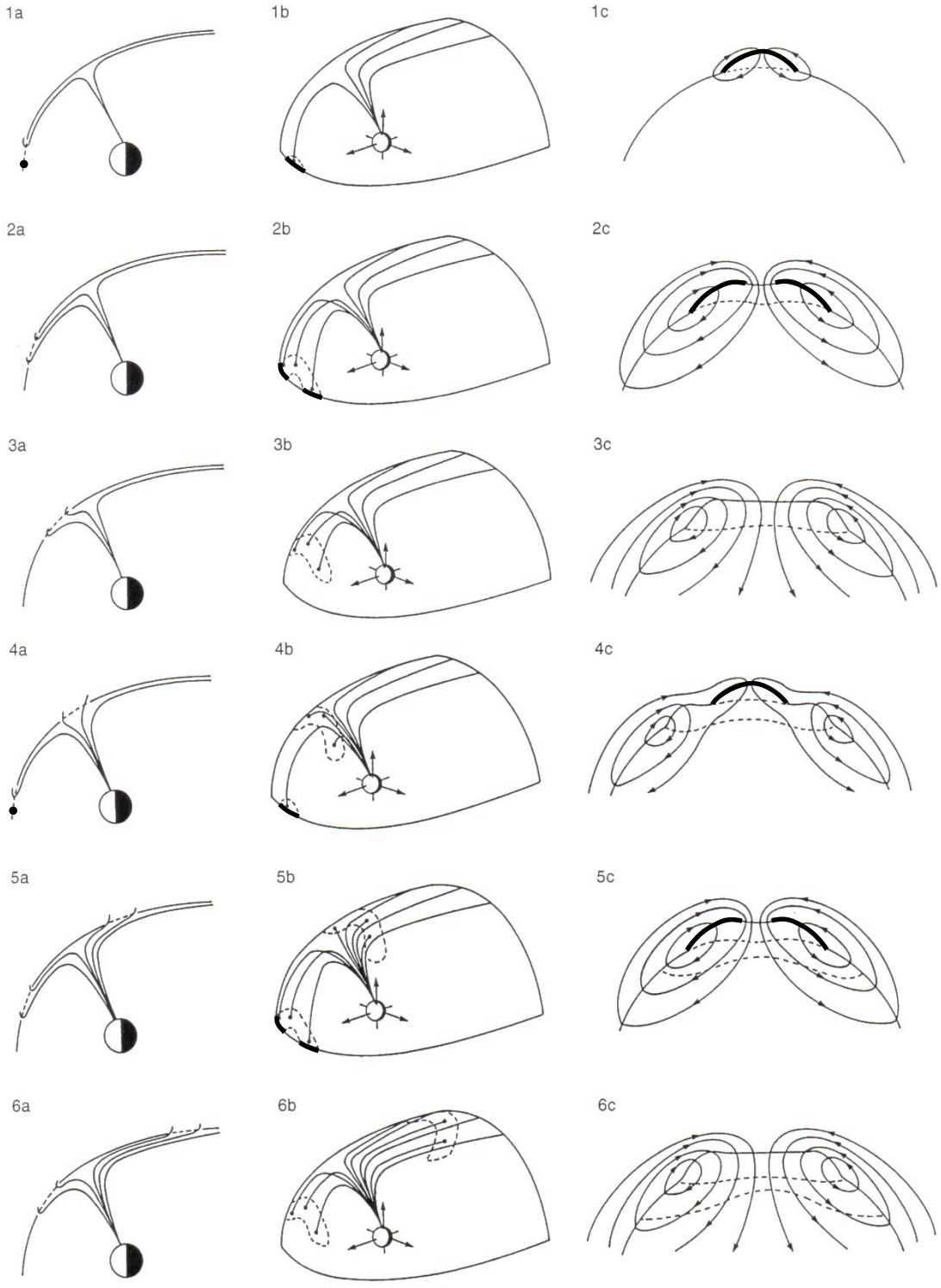

Fig. 2. The effects of pulsed reconnection at the magnetopause and in the ionosphere. The three columns show: **a** (*left*) a noon-midnight cross section of the magnetopause; **b** (*middle*) a view of the magnetosphere from the mid-latitudes in the mid-afternoon sector; and **c** (*right*) a view of the dayside ionosphere with noon at the top. Reconnection pulses 1 min long and every 4 min commence at $t = 0$. *Rows* are for t of 1, 2, 3, 4, 5 and 6 min (*top to bottom*) (after Lockwood, 1994)

same manner as did the onset of reconnection. Hence at any one MLT, the reconnection lasts for 1 min. Figure 2(2a) shows the reconnection at $t = 2$ min has ceased at noon, but 2(2b) shows that it is still ongoing at MLT on either side of noon. As the patch of newly opened flux moves over a magnetopause satellite, the two-dimensional theories predict that an FTE signature would be seen (Southwood *et al.*, 1988; Scholer, 1988, 1989; Semenov *et al.*, 1991, 1992). (N.B. at this time, away from noon where the reconnection continues, the FTE would be coated with streaming electrons from the active reconnection X-line whereas at noon such electrons would be absent). At noon, the ionospheric open/closed boundary is now equatorward of its zero flow equilibrium location, for the amount of open flux that exists at this time. Conversely, nearer dawn and dusk, the boundary is poleward of the equilibrium location at that instant. Hence, flow of the kind shown in Fig. 2(2c) will be excited as the system tends towards the new equilibrium. At noon the polar cap boundary is now adiaroic ($V' = 0$) and moving poleward ($V_c = V_b > 0$); at MLT beyond the active merging gaps the flow is weakly equatorward ($V' = 0$; $V_c = V_b < 0$). Equatorward of the open/closed boundary in both the morning and afternoon sectors, an increase in sunward flow propagates antisunward with the active merging gap segment, as reported by Lockwood *et al.* (1986; 1993c) and Moen *et al.* (1996).

In Fig. 2, the reconnection pulse is not shown as expanding beyond the mid-morning and mid-afternoon sectors, although magnetopause observations do indicate that reconnection at low latitudes can extend beyond these points. Figure 2(3a) and 2(3b) shows a situation at time $t = 3.5$ min where reconnection has ceased at all MLT. It should be noted that if the travelling reconnection enhancement persists for longer, it is possible that the next reconnection pulse begins before the prior one has disappeared and the situation illustrated here for time $t = 3$ min may never occur. The patch of RD produced by the burst of reconnection is now evolving over the dayside magnetopause. Each newly opened field line will evolve according to the magnetic tension and magnetosheath flow it experiences and both, and hence the pattern of motion, will depend upon the MLT. Therefore the patch of RD (and any associated FTE structure) will change in shape as it evolves. Figure 2(3c) shows that at this time, (3 min after the reconnection onset) flows are approaching their peak speed, even though there is now no reconnection present at any MLT. The time constant for the subsequent decay of this flow is of the order of 15 min, that being the time for the magnetosphere to approach equilibrium with less flux on the dayside and a flared tail (the transfer of flux into the tail by the magnetosheath flow taking of order this time). Hence, even where no reconnection pulse to follow the first, there would be (decaying) ionospheric flow for approximately a further 15 min.

At times 4–5 min, the second reconnection pulse takes place at noon, and the subsequent behaviour is as for the previous pulse. However, Fig. 2(4a–6a) and 2(4b–6b) is not the same as the corresponding figures in the previous cycle [Fig. 2(1a–3a) and 2(1b–3b)], only in that the second patch of RD forms and evolves over the dayside while the first is still evolving into the tail lobe. Note that the magnetopause has become antisunward-moving patches of RD, separated by extensive regions of TD: the ratio of the areas of RD and TD in the high-latitude boundary layer being the mark-space ratio of the reconnection pulses (in this example 1/4.5. Likewise, Fig. 2(4c–6c) is not the same as the flow patterns shown in Fig. 2(1c–3c): the flows caused by the second burst of reconnection are superposed on the residual flows due to the prior pulse of reconnection.

One very important prediction of the above model is that each patch of newly opened flux in the ionosphere is appended directly sunward of the patch produced by the prior pulse. This happens because both the patches and the open-closed boundary evolve in shape. A boundary between the patches forms along the longitudinal extent of each patch and migrates poleward with the two patches it separates. This boundary marks a discontinuity in the variation of time-elapsed since reconnection with latitude. This leads to the prediction of steps in the cusp ion dispersion signatures, as explained in the following section. However, this is not the only explanation, as is also discussed in the following section.

The model of the effects of magnetopause reconnection bursts shown in Fig. 2 was put forward by Lockwood *et al.* (1993c) to explain radar and optical observations and predicts longitudinally extensive poleward-moving events, separated by longitudinally extensive cusp ion steps. However it does not place any limits on how extensive they are. However, there are some points to note about this model. It has not invoked a reconnection pulse which occurs simultaneously over a wide range of MLT, a concept to which Newell and Sibeck (1993) objected. Figure 2 demonstrates how it is not necessary to have such a pulse to form a longitudinally extensive event in the ionosphere. This is because the pulse can travel around the magnetopause, continuously adding to the ionospheric patch. However, at any one point on the X-line, the reconnection occurs only in one short-lived burst and at any point on the magnetopause, boundary-normal field is moved over a satellite only in patches of RD between regions of TD.

3 Spatial and temporal origins of cusp steps

Lockwood and Smith (1992, 1994) and Lockwood (1995b) discuss how the cusp ion precipitation characteristics are a function of the time elapsed since the field line was reconnected. Cusp ion steps arise from discontinuous changes in this elapsed time. Such changes can occur because of either spatial or temporal variations of the reconnection rate, as demonstrated in Fig. 3. Figure 3a shows a step, intersected by the satellite S at the point p, which arises between the steady-state flow streamlines emanating from two active reconnection X-lines, mapping to ionospheric merging gaps, A and B. Figure 3b shows a temporal explanation of the same step and flows derived from the discussion in the previous section. The numbered patches delineated by dotted lines are regions of newly

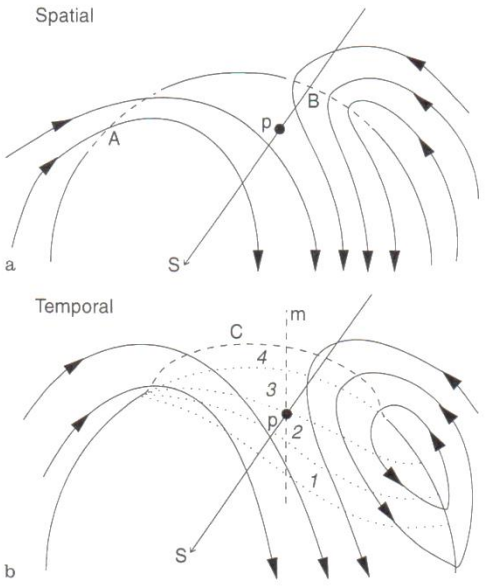

Fig. 3. **a** Spatial and **b** temporal explanations of a cusp ion step at p. For both figures, *noon* is at the *top*. *Dashed* and *solid lines* show reconnecting and adiaroic segments of the open/closed boundary; *lines* with *arrows* are flow streamlines and *dotted lines* in **b** delineate patches produced by reconnection pulses 1–4. **b** Is for the time t_{s1} in Fig. 5 (after Lockwood, 1995a).

opened flux, each produced by a reconnection burst. These occur in the order 1–4 at a magnetopause X-line which maps to the single merging gap C: the step at p arises because the patch 2 was reconnected at an earlier than patch 3. In Fig. 3b, the patch of flux opened by the most-recent burst (4) is seen as an equatorward extrusion of the open field line region. This, like the previous events, subsequently migrates poleward as the magnetosphere-ionosphere system evolves towards equilibrium with the new amount of open flux, as discussed in the previous section. Patches produced by earlier pulses (3, 2 and 1) are immediately poleward of patch 4, each being appended directly equatorward of that due to the prior pulse. The poleward motion of the cusp ion steps, and of the events between them, is predicted by the temporal but not the spatial model.

Onsager *et al.* (1995) and Weiss *et al.* (1995) have presented examples of steps which appear to be spatial in origin. In the case reported by Onsager *et al.* (1995), the step is seen at roughly the same latitude by two craft intersecting the cusp roughly 20 min apart. This could be coincidence and raises questions about the uncertainties of field line mapping, because the satellites were at different altitudes. Possibly more telling is the fact that the low-altitude satellite saw an upward step of a kind which would require the satellite to be moving along the open-closed boundary for the temporal explanation (so that $V_c > V_s$), which is very unlikely as the pass was meridional. On the other hand, the steps reported by Lockwood *et al.* (1993a) and Pinnock *et al.* (1995) are important because they were observed in very close conjunction with poleward-moving events, seen by the EISCAT and Halley Bay PACE radars. Other arguments that these examples of steps are temporal and not spatial are presented by Lockwood (1995a) and Lockwood *et al.* (1995c). This strongly implies a temporal origin of these events. However, as discussed in the introduction, interesting questions still arise about the spatial extent of the reconnection.

4. A model of cusp ion steps

The cusp ion spectrum is predicted here using the two-dimensional model of Lockwood (1995b) and as a function of time elapsed since the field line was reconnected $(t_s - t_o)$, where t_s is the observation time and t_o is the time that the field line observed was reconnected. This model is similar in principle to that employed by Onsager *et al.* (1993; 1995) but has a significant advantage for the present study in that the input reconnection rate may be pulsed (Lockwood and Smith, 1994). We here assume the reconnection is at the subsolar point. The magnetosheath field points south so that the newly opened field lines evolve antisunward along a streamline in the noon-midnight plane. All other details, such as solar wind conditions, magnetopause Alfvén speed, RD angles and field-aligned distance from the magnetopause to the ionosphere are as given by Lockwood (1995b). It is not necessary to assume magnetic and electric field distributions in the dayside magnetosphere, but it is assumed that the reconnection rate variations do not alter the field-aligned distance from any one point on the magnetopause to the ionosphere.

Figure 4a shows the modelled differential energy flux as a function of energy and $(t_s - t_o)$. A feature to note is the time-of-flight low-energy cut-off of the ion spectra. For elapsed times up to $(t_s - t_o) = 75$ s, these minimum-energy ions have all come from near the X-line (Lockwood and Smith, 1992; Lockwood *et al.*, 1995c); after this time they come from close to the magnetic cusp. The origin of the small spur-like feature at $(t_s - t_o) = 75$ s has been discussed by Lockwood (1995b).

In order to calculate the sequence of spectra that will be seen by a satellite, we must calculate the $(t_s - t_o)$ of the field lines that it intersects, as a function of observing time, t_s. Figure 4a can then be used to determine the spectrum detected as a function of t_s.

Figure 5 illustrates how this is done: the upper panel shows the assumed input square wave variation of the reconnection rate, E_t; the lower panel shows the location of flux tubes with x being the poleward direction, normal to the ionospheric merging gap (e.g. along the meridian marked m in Fig. 3). The period of the reconnection rate variation used here is $T = 4$ min and between each pulse $dt = 1$ min long, the reconnection rate falls to zero. These are close to the mode values of the distributions of both magnetopause FTEs (Lockwood and Wild, 1993) and poleward-moving auroral transients (Fasel, 1995). The poleward flows excited will be inductively smoothed, with a time constant of order 15–20 min. In this work, we assume that the smoothing is complete such that the poleward flow speed has a constant V_c, corresponding to the mean reconnection rate. The effects of a remnant

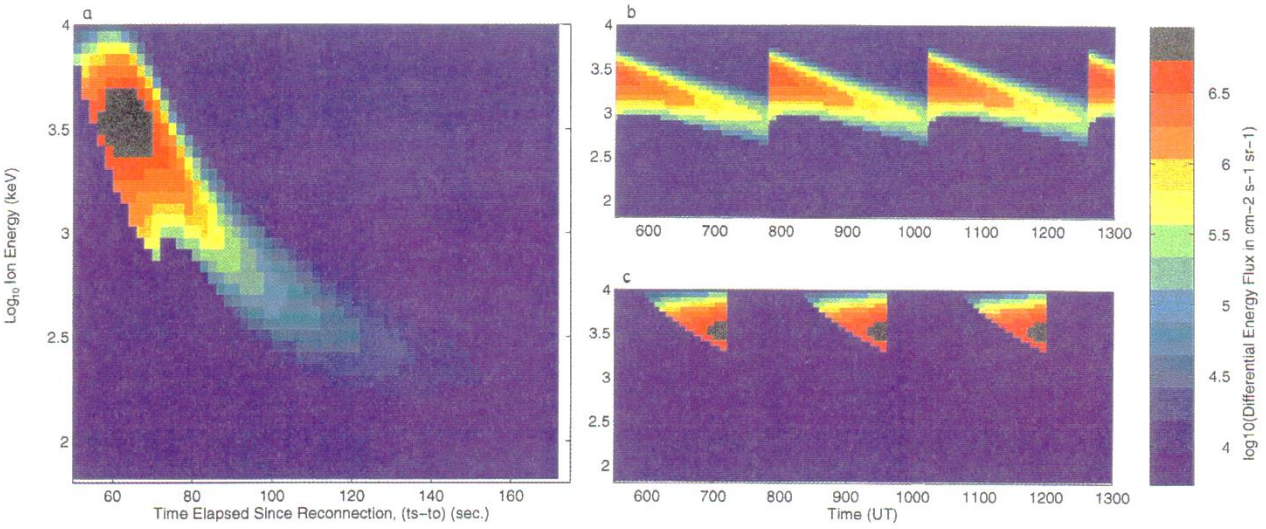

Fig. 4a–c. Modelled energy-time spectrograms of different energy flux; **a** as a function of time elapsed since reconnection ($t_s - t_o$); and **b** a function of observation time t_s for pass B and **c** pass C in Fig. 5

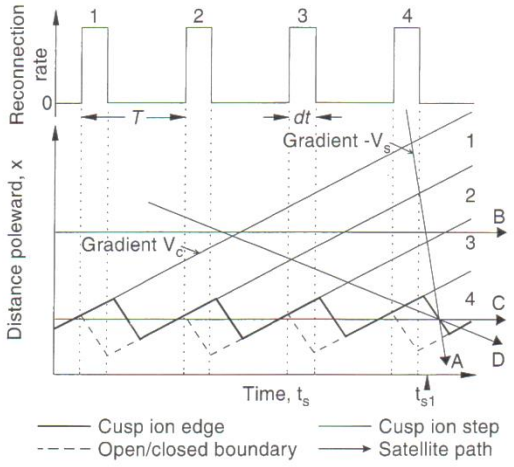

Fig. 5. The reconnection rate variation (*top*) and position along the meridian m in Fig. 3, x (*bottom*), as a function of time, t_s, of: cusp ion steps (*thin solid lines*); the open/closed field line bpundary (*dashed line*); the ion edge (*thick solid line*) and the satellite, for passes with orientations *A-D* (*arrows*)

ripple (of period T) in the poleward flow speed will be discussed later. The dashed line is the open-closed field line boundary: during the reconnection pulse, the boundary erodes equatorward at speed $|V_b|$, given by Eqs. (2) and (3) to be $|V_c - (\varepsilon/B_i)\cdot(dy'/dy)|$, whereas between the pulses the boundary becomes adiaroic and relaxes back poleward with the convection speed V_c. For simplicity, we here assume that there is no drift in the boundary location in each period T, so that $<V_b>$ is zero, giving the (constant) value of V_c:

$$V_c = (<\varepsilon>/B_i)\cdot(dy'/dy) = (\varepsilon_p/B)\cdot(dy'/dy)\cdot(dt/T), \qquad (4)$$

where ε_p is the value of the reconnection rate within the pulses. We here set V_c to be 500 m s^{-1}, which means that V' is equal to 2 km s^{-1} during the reconnection pulses [corresponding to a reconnection rate of ε_p of 3.3 mV m^{-1} within the pulses for a typical (dy'/dy) of 30]. This means that V_b within the pulses is -1.5 km s^{-1} and in their duration of $dt = 60$ s the boundary migrates equatorward by 90 km, or almost 1 degree of latitude. If the model variations in reconnection rate applied over a distance of 1000 km (see Sect. 6), then the mean reconnection voltage would be 25 kV, all of which is contributed by the pulses despite only being present at any one MLT for a quarter of the time.

The solid line in the lower panel of Fig. 5 is the ion edge, where fluxes of magnetosheath ions exceed the instrument detection threshold: it lies at a time elapsed since reconnection equal to the time-of-flight of the most energetic ions injected at the X-line with detectable flux (Gosling *et al.*, 1990). The reconnection pulses 1–4 generate the patches of newly opened flux 1–4, the boundaries between which (i.e. cusp ion steps) are shown in Fig. 5 moving poleward at V_c. Note that Fig. 3b is a snapshot for the time t_{s1} in Fig. 5. Figure 5 also shows the loci of four satellites, A, B, C and D. These differ in their value of $V_s = dx/dt_s$. In the next section we consider the cusp ion energy-time spectrogram seen by each. For any point (x, t) in Fig. 5, the time elapsed since reconnection $(t_s - t_o)$ is proportional to the length of the flow streamline from (x, t) back to where it intersected the open/closed boundary.

5 Modelled cusp ion spectrograms

Satellite A in Fig. 5 is moving meridionally equatorward ($V_s < 0$). As it crosses each patch of newly opened flux $(t_s - t_o)$ decreases: from Fig. 4a, this will result in an upward ramp of the lower cut-off energy and of contours of constant differential energy flux. As it crosses between two patches $(t_s - t_o)$ decreases discontinuously, giving an upward step in the spectrogram. On emerging from event 4, the satellite remains equatorward of the ion edge and no

more magnetosheath ions are detected. Figure 6a shows the spectrogram modelled for such a pass. The details can be varied by altering the phase of the satellite pass, relative to the cycle of the reconnection rate variation. The phasing used here is chosen to provide a spectrogram similar (in general form rather than in detail) to the data shown in Fig. 6b (from Lockwood *et al.*, 1993a). The form of the cusp ion steps is as predicted in Fig. 10d of Lockwood and Smith (1994).

Satellite B in Fig. 5 has $V_s = 0$. As it traverses each patch $(t_s - t_o)$ increases and thus, from Fig. 4a, the ion energies fall with time. At the boundary between patches, the more recently reconnected patch is convected over the spacecraft causing $(t_s - t_o)$ to decrease discontinuously and giving an upward ion step. This behaviour was predicted in Fig. 10c of Lockwood and Smith (1994) and is shown in the modelled spectrogram in Fig. 4b. Pass C in Fig. 5 is also for $V_s = 0$, but is at a lower latitude and closer to the mean location of the open/closed boundary. In this case, the ion edge erodes equatorward across the satellite during the reconnection pulses, but then relaxes poleward across it again when the reconnection switches off between the pulses. The energy-time spectrogram modelled is shown in Fig. 4c. In this one case only, the pulsed reconnection does lead to a pulsed appearance on the cusp ion spectrogram. It is unlikely that this sequence would be observed for more than a few cycles as this would require the satellite to maintain a constant separation with the mean location of the open-closed boundary.

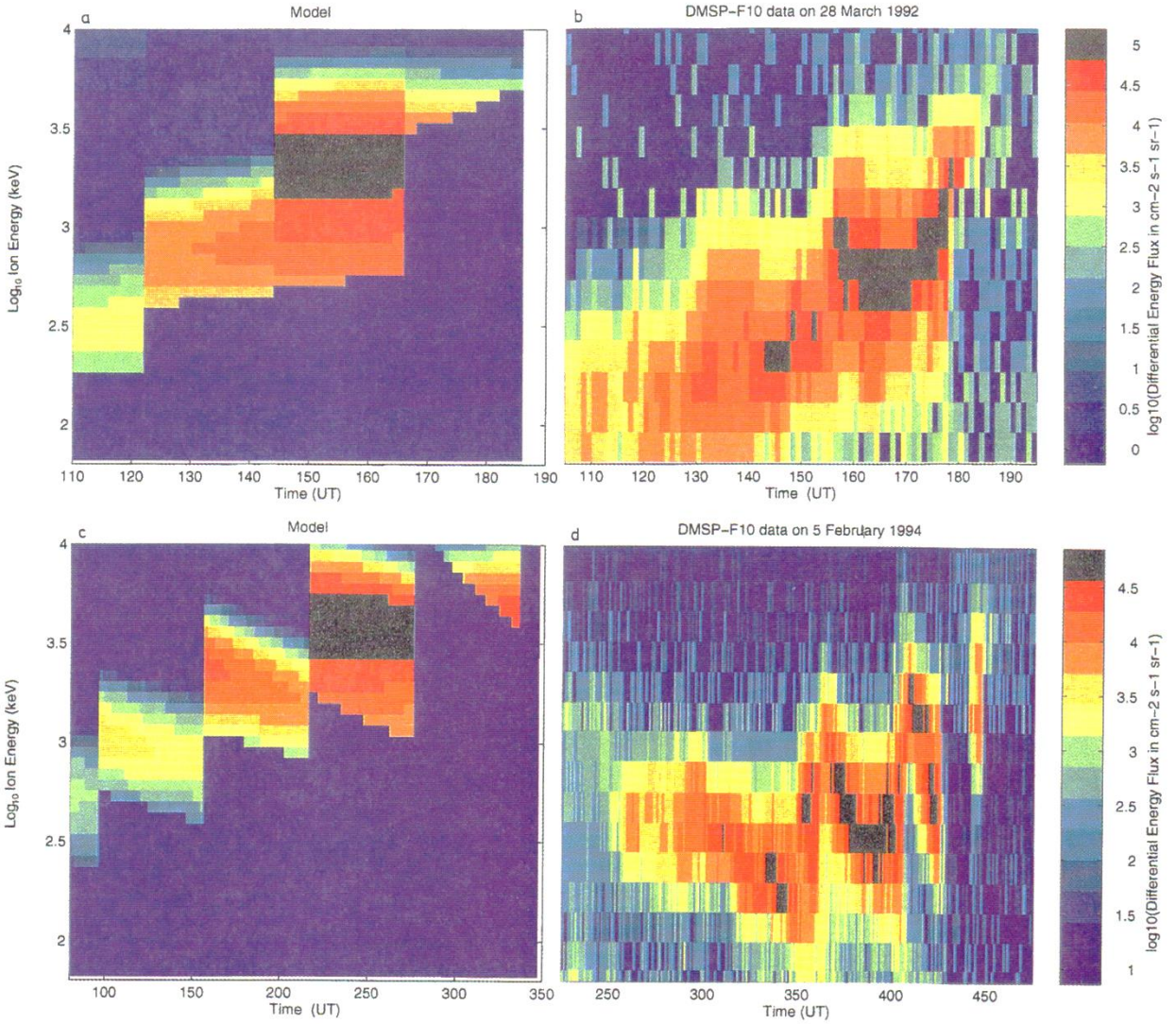

Fig. 6a–d. Modelled and observed energy-time spectrograms of differential energy flux for **a** a meridionally moving satellite (pass A in Fig. 5) such as **b** DMSP-F10 on 28 March 1992 ($t_s = 0$ at 10:08) (see Lockwood *et al.*, 1993a); **c** a longitudinally moving satellite (pass D in Fig. 5) such as **d** DMSP-F8 on 5 February 1994 (see Pinnock *et al.*, 1995)

Satellite D in Fig. 5 moves equatorward, but with much smaller speed $|V_s|$ than satellite A. This case applies to a longitudinal spacecraft orbit, which is slowly approaching the mean location of the open-closed boundary. The satellite moves from a situation like that shown in Fig. 4b, to one like that shown in Fig. 4c, prior to emerging equatorward of the cusp/cleft region. The spectrogram predicted for such a pass is shown in Fig. 6c. The model produces cusp ion dispersion which is similar to that reported by Pinnock *et al.* (1995) and reproduced here in Fig. 6d. The important feature to notice is that Fig 6a and 6c are for essentially the same sets of geophysical conditions and that the differences between them arise purely because of the orientation of the satellite orbit. In modelling the observed steps, only the phase of the satellite pass was varied. Parts (a) and (c) of Fig. 6 are thus not intended to be close matches to the corresponding data (parts b and d respectively) and there is little doubt that a closer and more detailed match between observation and model could be achieved in each case by fine tuning the many inputs which could be varied to the model. However, there are sufficient inputs that little is to be learned from such an exercise and we wish here to highlight only some broad principles from the comparisons in the following section. It is also important to note that the model is two-dimensional and that we have therefore assumed that there are no longitudinal variations. Therefore we have, thus far, demonstrated that the data may be explained by reconnection which is temporally sporadic but not spatially patchy.

6 Comparison of modelled and observed cases

Figure 6a shows a clear upward step in the modelled lower cut-off ion energy at the observation time, $t_s = 168$ s. At this step, the peak detectable ion energy remains roughly constant. This is therefore similar to the step observed on 28 March 1992 at $t_s = 178$ s, where $t_s = 0$ is defined as being 10:08 UT in this case (Fig. 6) (see Lockwood *et al.*, 1995c for a detailed study of this step). At $t_s = 145$ s during this pass, on the other hand, the model predicts a step up in the peak detectable energy, with no detectable step in the lower cut-off energy. This is therefore similar to the step observed between $t_s = 153$ and 156 s in Fig. 6b. The model predicts a step in both peak and minimum detected energy at $t_s = 122$ s: this is observed for the peak energy at $t_s = 128$–132 s in Fig. 6b, but the step in the minimum energy is out of the range of the instrument. The predictions show increases in the differential energy flux across each step which are indeed present in Fig. 6b, albeit slightly smaller in amplitude. There are a number of ways in which the model could be adjusted to match the observations more closely in this respect. One of the simplest would be to move the reconnection site longitudinally away from the subsolar point so that the gradient in magnetosheath density along the flow streamline, followed by the newly opened field lines, is less steep.

The step observed at $t_s = 178$ s is instantaneous for several energy channels of the instrument (Lockwood *et al.*, 1995c), showing that the reconnection rate fell to zero between the two pulses. However, the other two steps are not instantaneous, showing that the reconnection rate fell to a small, but non-zero, value in the other gaps between the pulses (Lockwood and Smith, 1994). It is here worth noting the differences between two independent studies of these data which have appeared in the literature. The analysis of Lockwood *et al.* (1995c) of the step at $t_s = 178$ s shows that the cut-off energy rose from below 0.14 keV to over 1.38 keV in less than one 1-s instrument cycle: this is directly demonstrated by their Fig. 4 which shows that the flux decayed exactly simultaneously in the energy channels at 0.14, 0.206, 0.3, 0.44, 0.65, 0.955 and 1.38 keV. Thus, the step cannot be smaller than they state. They then derived a field-aligned distance from the satellite to the reconnection X-line of $d = 14.5 \pm 2\ R_E$ by matching this step in energies to the timing of the corresponding events seen by the ground-based EISCAT radar, yielding a period of zero (i.e., undetectable) reconnection rate lasting 6.4 ± 0.9 min. This is considerably longer than any of the periods of zero reconnection rate in the survey by Newell and Meng (1995b), who found none lasting longer than 2.5 min. These authors used the same technique to derive the cut-offs as Newell and Meng (1995a) and we can compare directly the analysis by Lockwood *et al.* (1995c) with that of the same step by Newell and Meng (1995a), who determined it was between energies of 300 eV and 679 eV only. Using the d of 10 R_E adopted by Newell and Meng (1995b), the step they inferred yields a period of zero reconnection rate lasting just 1.5 min. The difference is partly due to the lower value of d, but mainly because of the method used to derive the cut-offs by Newell and Meng yields a much small energy step. The technique of Newell and Meng determines a cut-off for each 1-s spectrum, a method which has several problems, as demonstrated by Lockwood (1995b) and Lockwood and Davis (1996). The analysis of Lockwood *et al.* (1995c) leaves no doubt that the step is much larger than derived by Newell and Meng (1995a), which indicates that the same technique will have caused Newell and Meng (1995b) to substantially underestimate the duration of periods of zero reconnection rate in their survey.

A significant difference between Fig. 6a and 6b is that the data show minima in the energy of flux contours mid-way between each step. This is not present in the model because of the assumption that the convection speed V_c is constant. The EISCAT radar data, taken in very close conjunction with these satellite data (see Lockwood *et al.*, 1993a) reveal the poleward flow speed is enhanced by about 100 m s^{-1} (over a steady level of about 400 m s^{-1}) at the poleward edge of each event (and thus immediately equatorward of each step). This causes a decrease in the ratio V_s/V_c on the equatorward side of each step, turning the upward ramp of the flux contours into a downward ramp with increasing t_s. Note that changes in V_c have a large effect on the data for 28 March 1992 because the satellite was moving at an angle of about 45° to the L shells, making $|V_s|$ smaller than for a purely meridional pass. The range of MLT covered by the satellite is significant, but relatively small: the first step is observed at an MLT which is 0.8 h greater than

the point where the satellite emerges through the ion edge.

In Fig. 6c, the ion energies are always higher in any patch than they were at the corresponding point of the previous patch, because the satellite has moved closer to the open/closed boundary. The subsequent ramp in ion energies is also steeper than it was for the previous patch. Both these features are seen in the data for 5 February 1994 (Fig. 6d). In these data, there are clear upward steps at $t_s = 350$–365 s (where $t_s = 0$ is defined to be at 10:36 UT for this case) and 400–410 s and probably a small one at 285–295 s. A feature clearly seen in both 6c and 6d is the passage of the ion edge over the satellite so that an isolated patch of ions is subsequently detected when the satellite briefly returns to poleward of the ion edge. This isolated patch, seen just before $t_s = 450$ s, was interpreted by Pinnock *et al.* (1995) as showing that the reconnection was patchy, but is here modelled by assuming temporal reconnection, with no spatial structure. The first three steps in the data are all not instantaneous thus, as in Fig. 6b, the reconnection rate fell to a very low, but non-zero, values between the pulses.

The modelled differential energy flux increases across each step. Such changes are seen across the first and second steps but not the third. We would expect longitudinal variations in the magnetosheath density to be convolved with the changes predicted here due to changes in $(t_s - t_o)$. The magnetosheath-like ion precipitation in Fig. 6d extends over roughly 3 h of MLT and this could map to an even greater extent on the magnetopause. This would give significant longitudinal change in the sheath densities which has not been allowed for by the 2-dimensional model presented here.

The model predicts the general form of the cusp ion spectrogram by neglecting longitudinal variations which shows that, for the temporal explanation, the events are longitudinally extensive, and cover at least the 3 h of MLT that the satellite giving the data shown in Fig. 6d remained in the region of sheath-like precipitation. As discussed in Sect. 2, this does not necessarily imply that the reconnection pulse generating each patch is simultaneous over this longitudinal extent. The pulse may travel in MLT, such that the rate at any one MLT shows the variation in Fig. 5. This will result in some longitudinal, as well as latitudinal, variations in $(t_s - t_o)$ within each event.

From this, we can conclude that the time series of cusp ions detected by Pinnock *et al.* (1995) could be exactly the same phenomenon as that reported by Lockwood *et al.* (1993a), the different character of the steps in the two cases being due to the direction of satellite motion which determines the ratio of the satellite and convection velocities normal to the open/closed boundary, V_s/V_c. The isolated patch of ion precipitation seen by the satellite is well explained by this purely temporal model and does not necessarily imply a spatial patch, as was invoked by Pinnock *et al.* (1995). We can therefore state that there is no need to invoke spatial structure to explain these data, in addition to the temporal variations. However, in the remainder of this section we argue that the evidence strongly suggests that such spatial structure is either absent or, if present, is part of event evolution in a manner exemplified by Fig. 2.

Firstly, for time varying reconnection at different sites which are fully independent of each other, the repetition rate of pulses will, in general, be different at each site and there would be no fixed phase relationship between the pulses produced at these different sites. Thus, as the satellite travelled longitudinally and crossed from patches produced by one reconnection site to those produced by another, cusp ion steps which are upward would be as common as those that are downward. This is not the case here, all steps being upward. Indeed, the steps are not only all upward, but each is to a higher energy than the previous one. Figure 6c shows that this is expected for the temporal model but, from the earlier explanation cannot be expected for temporal and spatial models. Furthermore, within each patch the slope of the downward ion dispersion between each step would increase if the satellite were moving away from the reconnection site. This is also inconsistent with the data in Fig. 6d, where the slope of the dispersion between the steps is lowest initially and subsequently increases; despite the fact that the satellite is drifting poleward before $t_s = 350$ s, but is at roughly constant magnetic latitude after this time.

The regular progression of the steps in Fig. 6d (with peak energies and the slope of the ramps increasing for events seen closer to the open/closed boundary) is only explained by the temporal model alone: a sporadic and patchy reconnection explanation needs to explain why the pulses of reconnection at the spatially separated active X-lines had the coherent phase relation needed to produce the observed variation. The model of travelling active X-line segments, introduced by Lockwood *et al.* (1993c) to explain observations and demonstrated here in Fig. 2, does allow spatial structure in the reconnection to exist at any one time and yet also generates the coherent phase relationship needed to explain the cusp ion steps shown in Fig. 6c, d. However, we can eliminate isolated active X-lines which reconnect sporadically as a cause of these events.

The results presented here therefore strongly imply that the reconnection pulses extend (although not necessarily at any one instant of time, as demonstrated by Fig. 2) over a range of MLT of at least 3 h. This is a minimum estimate because the extent of the events was not fully defined by the satellite owing to the fact that it was equatorward of the ion edge after $t_s = 450$ s. This corresponds to ionospheric patches in excess of about 1000 km in longitudinal extent as reported by Lockwood *et al.* (1990; 1993b) and Pinnock *et al.* (1993). We would therefore argue that the poleward-moving events seen by the Halley Bay radar by Pinnock *et al.* (1995) are very likely to have been the same events as were seen passing over the DMSP satellite at a different MLT.

Acknowledgements. The authors are supported by the UK Particle Physics and Astronomy Research Council. We are grateful to F. Rich of Phillips Laboratory for supplying us with the DMSP F8 ion precipitation data and S. W. H. Cowley, M.F. Smith and T. Onsager for helpful discussions of this work.

The Editor-in-Chief thanks T. Onsager and P. Reiff for their help in evaluating this paper.

References

Biernat, H. K., M. F. Heyn, and V. S. Semenov, Unsteady Petschek reconnection, *J. Geophys. Res.*, **92,** 3392–3396, 1987.

Burch, J. L., Rate of erosion of dayside magnetic flux based on a quantitative study of polar cusp latitude on the interplanetary magnetic field, *Radio Sci.*, **8,** 955–961, 1973.

Coroniti, F. V., and C. F. Kennel, Can the ionosphere regulate magnetospheric convection?, *J. Geophys. Res.*, **78,** 2837–2851, 1973.

Cowley, S. W. H., and M. Lockwood, Excitation and decay of solar wind-driven flows in the magnetosphere-ionosphere system, *Ann. Geophysicae*, **10,** 103–115, 1992.

Cowley, S. W. H., M. P. Freeman, M. Lockwood, and M. F. Smith, The ionosphere signature of flux transfer events, in '*CLUSTER – dayside polar cusp*', Ed. C. I. Barron, ESA SP-330, 105–112, European Space Agency, Nordvijk, The Netherlands, 1991.

Crooker, N. U., Reverse convection, *J. Geophys. Res.*, **97,** 19,363–19,372, 1992.

Denig, W. F., W. J. Burke, N. C. Maynard, F. J. Rich, B. Jacobsen, P. E. Sandholt, A. Egeland, S. Leontjev, and V. G. Vorobjev, Ionospheric signatures of dayside magnetopause transients: a case study using satellite and ground measurements, *J. Geophys. Res.*, **98,** 5969–5980, 1993.

Elphic, R. C., M. Lockwood, S. W. H. Cowley, and P. E. Sandholt, Signatures of flux transfer events at the dayside magnetopause and in the ionosphere: combined ISEE, EISCAT and optical observations, *Geophys. Res. Lett.*, **17,** 2241–2244, 1990.

Escoubet, C. P., M. F. Smith, S. F. Fung, P. C. Anderson, R. A. Hoffman, E. M. Basinska and J. M. Bosqued, Staircase ion signature in the polar cusp: a case study, *Geophys. Res. Lett.*, **19,** 1735–1738, 1992

Etemadi, A., S. W. H. Cowley, M. Lockwood, B. J. I. Bromage, D. M. Willis, and H. Lühr, The dependence of high-latitude dayside ionospheric flows on the north-south component of the IMF, a high time resolution correlation analysis using EISCAT "POLAR" and AMPTE UKS and IRM data, *Planet. Space Sci.*, **36,** 471–498, 1988.

Fasel, G. J., Poleward-moving auroral forms: a statistical study, *J. Geophys. Res.*, **100,** 11891–11899, 1995.

Foster, J. C., G. S. Stiles, and J. R. Doupnik, Radar observations of cleft dynamics, *J. Geophys. Res.*, **85,** 3453–3460, 1980.

Freeman, M. P., C. J. Farrugia, L. F. Burlaga, M. R. Hairston, M. E. Greenspan, J. M. Ruohoniemi, and R. P. Lepping, The interaction of a magnetic cloud with the earth: ionospheric convection in the northern and southern hemispheres for a wide range of quasi-steady interplanetary magnetic field conditions, *J. Geophys. Res.*, **98,** 7633–7655, 1993.

Freeman, M. P., and D. J. Southwood, The effects of magnetospheric erosion on mid- and high-latitude ionospheric flows, *Planet. Space Sci.*, **36,** 509–522, 1988.

Gosling, J. T., M. F. Thomsen, S. J. Bame, T. G. Onsanger and C. T. Russell, The electron edge of the low-latitude boundary layer during accelerated flow events, *Geophys. Res. Lett.*, **17,** 1833–1836, 1990.

Hapgood, M. A., and M. Lockwood, Rapid changes in LLBL thickness, *Geophys. Res. Lett.*, **22,** 77–80, 1995.

Holzer, T. E., and G. C. Reid, The response of the dayside magnetosphere-ionosphere system to time-varying field-line reconnection, *J. Geophys. Res.*, **80,** 2041–2049, 1975.

Horwitz, J. L., and S.-I. Akasofu, The response of the dayside aurora to sharp northward and southward transitions of the interplanetary magnetic field and to magnetospheric substorms, *J. Geophys. Res.*, **82,** 2723–2734, 1977.

Knipp, D. J., B. A. Emery, A. D. Richmond, N. U. Crooker, M. R. Hairston, J. A. Cumnock, W. F. Denig, F. J. Rich, O. del la Beaujardiere, J. M. Ruohoniemi, A. S. Rodger, G. Crowley, B.-H. Ahn, D. S. Evans, T. J. Fuller-Rowell, E. Friis-Christiansen, M. Lockwood, H. Kroehl, C. McClennan, A, McEwin, R. J. Pellinen, R. J. Morris, G. B. Burns, V. Papitashvili, A. Zaitzev, O. Troshichev, N. Sato, P. Sutcliffe, and L. Tomlinson, Ionospheric convection response to strong, slow variations in a northward interplanetary magnetic field: A case study for January 14, 1988, *J. Geophys. Res.*, **98,** 19,273–19,292, 1993.

Lockwood, M., Ionospheric signatures of pulsed magnetopause reconnection, in Physical signatures of magnetopause boundary layer processes, Ed. J. A. Holtet and A. Egeland, NATO ASI Series C, vol. 425, Kluwer, 229–243, 1994.

Lockwood, M., Ground-based and satellite observations of the cusp: evidence for pulsed magnetopause reconnection, in *Physics of the magnetopause*, Ed. P. Song, B. U. O. Sonnerup and M. Thompsen, American Geophysical Union Monograph 90, 417–426, 1995a.

Lockwood, M., The location and characteristics of the reconnection X-line deduced from low-altitude satellite and ground-based observations: 1. Theory, *J. Geophys. Res.*, **100,** 21791–21802, 1995b.

Lockwood, M., and S. W. Cowley, Ionospheric convection and the substorm cycle, in *Substorms 1, Proceedings of the First International Conference on Substorms, ICS-1*, Ed. C. Mattock, ESA-SP-335, 99–110, European Space Agency Publications, Nordvijk, The Netherlands, 1992.

Lockwood, M., and S. W. H. Cowley, Comment on "Ionospheric signatures of dayside magnetopause transients: a case study using satellite and ground measurements" by Denig *et al.*, *J. Geophys. Res.*, **99,** 4253–4255, 1994.

Lockwood, M., and C. J. Davis, An analysis of the accuracy of magnetopause reconnection rate variations deduced from cusp ion dispersion characteristics, *Ann. Geophysicae*, **14,** 149–161, 1996.

Lockwood, M., and M. F. Smith, Low-altitude signatures of the cusp and flux transfer events, *Geophys. Res. Lett.*, **16,** 879–883, 1989.

Lockwood, M., and M. F. Smith, The variation of reconnection rate at the dayside magnetopause and cusp ion precipitation, *J. Geophys. Res.*, **97,** 14,841, 1992.

Lockwood, M., and M. F. Smith, Low- and mid-altitude cusp particle signatures for general magnetopause reconnection rate variations: I - Theory, *J. Geophys. Res.*, **99,** 8531–8555, 1994.

Lockwood, M., and M. N. Wild, On the quasi-periodic nature of magnetopause flux transfer events, *J. Geophys. Res.*, **98,** 5935–5940, 1993.

Lockwood, M., A. P. van Eyken, B. J. I. Bromage, D. M. Willis, and S. W. H. Cowley, Eastward propagation of a plasma convection enhancement following a southward turning of the interplanetary magnetic field, *Geophys. Res. Lett.*, **13,** 72–75, 1986.

Lockwood, M., P. E. Sandholt, S. W. H. Cowley, and T. Oguti, Interplanetary magnetic field control of dayside auroral activity and the transfer of momentum across the dayside magnetopause, *Planet. Space Sci.*, **37,** 1347–1365, 1989.

Lockwood, M., S. W. H. Cowley, P. E. Sandholt, and R. P. Lepping, The ionospheric signatures of flux transfer events and solar wind dynamic pressure changes, *J. Geophys. Res.*, **95,** 17,113–17,136, 1990a.

Lockwood, M., S. W. H. Cowley, and M. P. Freeman, The excitation of plasma convection in the high-latitude ionosphere, *J. Geophys. Res.*, **95,** 7961–7971, 1990b.

Lockwood, M., W. F. Denig, A. D. Farmer, V. N. Davda, S. W. H. Cowley, and H. Lühr, Ionospheric signatures of pulsed magnetic reconnection at the Earth's magnetopause, *Nature*, **361** (6411), 424–428, 1993a.

Lockwood, M., H. C. Carlson, and P. E. Sandholt, The implications of the altitude of transient 630-nm dayside auroral emissions, *J. Geophys. Res.*, **98,** 15571–15587, 1993b.

Lockwood, M., J. Moen, S. W. H. Cowley, A. D. Farmer, U. P. Løvhaug, H. Lühr, and V. N. Davda, Variability of dayside convection and motions of the cusp/cleft aurora, *Geophys. Res. Lett.*, **20,** 1011–1014, 1993c.

Lockwood, M., S. W. H. Cowley, M. F. Smith, R. P. Rijnbeek, and R. C. Elphic, The contribution of flux transfer events to convection, *Geophys. Res. Lett.*, **22,** 1185–1188, 1995a.

Lockwood, M., S. W. H. Cowley, P. E. Sandholt, and U. P. Løvhaug, Causes of plasma flow bursts and dayside auroral transients: an evaluation of two models invoking reconnection pulses and changes in the Y-component of the magnetosheath field, *J. Geophys. Res.*, **100,** 7613–7626, 1995b.

Lockwood, M., C. J. Davis, M. F. Smith, T. G. Onsager, and W. F. Denig, The location and characteristics of the reconnection X-line deduced from low-altitude satellite and ground-based observations: 2. DMSP and EISCAT radar data, *J. Geophys. Res.*, **100,** 21803–21814, 1995c.

Moen, J., P. E. Sandholt, M. Lockwood, W. F. Denig, U. P. Løvhaug, B. Lybekk, A. Egeland, D. Opsvik, and E. Friis-Christensen, Events of enhanced convection and related dayside auroral activity, *J. Geophys. Res.*, **100,** 23917–23934, 1995.

Moen, J., M. Lockwood, P. E. Sandholt, U. P. Løvhaug, W. F. Denig, A. P. van Eyken, and A. Egeland, Variability of dayside high-latitude convection associated with a sequence of auroral transients, *J. Atmos. Terr. Phys.*, **58,** 85–96, 1996.

Newell, P. T., and C.-I. Meng, Ion acceleration at the equatorward edge of the cusp: low-altitude observations of patchy merging, *Geophys. Res. Lett.*, **18,** 1829–1832, 1991.

Newell, P. T., and C.-I. Meng, Magnetopause dynamics as inferred from plasma observations on low-altitude satellites, in *Physics of the magnetopause*, Eds. P. Song, B. U. O. Sonnerup and M. Thompsen, American Geophysical Union Monograph 90, 407–416, 1995a.

Newell, P. T., and C.-I. Meng, Cusp low-energy ion cut-offs: a survey and implications for merging, *J. Geophys. Res.*, **100,** 21943–21951, 1995b.

Newell, P. T., and D. G. Sibeck, Upper limits on the contribution of flux transfer events to ionospheric convection, *Geophys. Res. Lett.*, **20,** 2829–2832, 1993.

Newell, P. T., and D. G. Sibeck, Magnetosheath fluctuations, ionospheric convection and dayside ionospheric transients, *In Physical Signatures of Magnetospheric Boundary Layer Processes*, J. A. Holtet and A. Egeland Eds, pp. 245–261, Kluwer, 1994.

Onsager T. G., C. A. Kletzing, J. B. Austin, and H. MacKiernan, Model of magnetosheath plasma in the magnetosphere: cusp and mantle particles at low altitudes, *Geophys. Res. Lett.*, **20,** 479–482, 1993.

Onsager, T. G., Shen-Wu Chang, J. D. Perez, J. B. Austin, and X. L. Janoo, Low-altitude observations and modelling of quasi-steady magnetopause reconnection, *J. Geophys. Res.*, **100,** 11831–11844, 1995.

Pinnock, M., A. S. Rodger, J. R. Dudeney, K. B. Baker, P. T. Newell, R. A. Greenwald, and M. E. Greenspan, Observations of an enhanced convection channel in the cusp ionosphere, *J. Geophys. Res.*, **98,** 3767–3776, 1993.

Pinnock, M., A. S. Rodger, J. R. Dudeney, F. Rich, K. B. Baker, High spatial and temporal resolution observations of the ionospheric cusp, *Ann. Geophysicae*, **13,** 919–925, 1995.

Pudovkin, M. I., S. A. Zaitseva, P. E. Sandholt, and A. Egeland, Dynamics of aurorae in the cusp region and characteristics of magnetic reconnection at the magnetopause, *Planet. Space Sci.*, **40,** 879–887, 1992.

Russell, C. T., and R. C. Elphic, Initial ISEE magnetometer results: magnetopause observations, *Space Sci. Rev.*, **22,** 681–715, 1978.

Sanchez, E. R., G. L. Siscoe, and C.-I. Meng, Inductive attenuation of the transpolar voltage, *Geophys. Res. Lett.*, **18,** 1173–1176, 1991.

Sandholt, P. E., M. Lockwood, W. F. Denig, R. C. Elphic, and S. Leontjev, Dynamical auroral structure in the vicinity of the polar cusp: multipoint observations during southward and northward IMF, *Ann. Geophysicae*, **10,** 483–497, 1992.

Saunders, M. A., Recent ISEE observations of the magnetopause and low-latitude boundary layer: a review, *J. Geophys.*, **52,** 190–198, 1983.

Saunders, M. A., M. P. Freeman, D. J. Southwood, S. W. H. Cowley, M. Lockwood, J. C. Samson, C. J. Farrugia, and T. J. Hughes, Dayside ionospheric convection changes in response to long-period interplanetary magnetic field oscillations: determination of the ionospheric phase velocity, *J. Geophys. Res.*, **97,** 19,373–19,380, 1992.

Scholer, M., Magnetic flux transfer at the magnetopause based on single X-line bursty reconnection, *Geophys. Res. Lett.*, **15,** 291–294, 1988.

Scholer, M., Asymmetric time-dependent and stationary magnetic reconnection at the dayside magnetopause, *J. Geophys. Res.*, **94,** 15099–15111, 1989.

Semenov, V. S., I. V. Kubyshkin, H. K. Biernat, M. F. Heyn, R. P. Rijnbeek, B. P. Besser, and C. J. Farrugia, Flux transfer events interpreted in terms of a generalized model for Petschek-type reconnection, *Adv. Space. Res.*, **11,** (9)25–(9)28, 1991.

Semenov, V. S., I. V. Kubyshkin, V. V. Lebedeva, R. P. Rijnbeek, M. F. Heyn, H. K. Biernat, and C. J. Farrugia, A comparison and review of steady-state and time-varying reconnection, *Planet. Space Sci.*, **40,** 63–87, 1992.

Siscoe, G. L., and T. S. Huang, Polar cap inflation and deflation, *J. Geophys. Res.*, **90,** 543–548, 1985.

Smith, M. F., M. Lockwood, and S. W. H. Cowley, The statistical cusp: a simple flux transfer event model, *Planet. Space Sci.*, **40,** 1251–1268, 1992.

Southwood, D. J., The ionospheric signature of flux transfer events, *J. Geophys. Res.*, **92,** 3207–3213, 1987.

Southwood, D. J., C. J. Farrugia, and M. A. Saunders, What are flux transfer events?, *Planet. Space Sci.*, **36,** 503–508, 1988.

Todd, H., S. W. H. Cowley, M. Lockwood, D. M. Willis, and H. Lühr, Response time of the high-latitude dayside ionosphere to sudden changes in the north-south component of the IMF, *Planet. Space Sci.*, **36,** 1415–1428, 1988.

Weiss, L. A., P. H. Reiff, H. C. Carlson, E. J. Weber, M. Lockwood, and W. K. Peterson, Flow-aligned jets in the magnetospheric cusp: results from the GEM pilot programme, *J. Geophys. Res.*, **100,** 7649–7660, 1995.

Woch, J., and R. Lundin, Temporal magnetosheath plasma injection observed with Viking: a case study, *Ann. Geophysicae*, **9,** 133–142, 1991.

Woch, J., and R. Lundin, Signatures of transient boundary layer processes observed with Viking, *J. Geophys. Res.*, **97,** 1431–1447, 1992.